Molecules and Cells

Gametophytic Abortion in Heterozygotes but Not in Homozygotes: Implied Chromosome Rearrangement during T-DNA Insertion at the *ASF1* Locus in *Arabidopsis*

Yunsook Min[1], Jennifer M. Frost[2,3], and Yeonhee Choi[1,*]

[1]Department of Biological Sciences, Seoul National University, Seoul 08826, Korea, [2]Department of Plant and Microbial Biology, University of California, Berkeley, CA 94720, USA, [3]Present address: Genomics and Child Health, Queen Mary University of London, London E1 2AT, United Kingdom
*Correspondence: yhc@snu.ac.kr
https://doi.org/10.14348/molcells.2020.2290
www.molcells.org

T-DNA insertional mutations in *Arabidopsis* genes have conferred huge benefits to the research community, greatly facilitating gene function analyses. However, the insertion process can cause chromosomal rearrangements. Here, we show an example of a likely rearrangement following T-DNA insertion in the *Anti-Silencing Function 1B* (*ASF1B*) gene locus on *Arabidopsis* chromosome 5, so that the phenotype was not relevant to the gene of interest, *ASF1B*. ASF1 is a histone H3/H4 chaperone involved in chromatin remodeling in the sporophyte and during reproduction. Plants that were homozygous for mutant alleles *asf1a* or *asf1b* were developmentally normal. However, following self-fertilization of double heterozygotes (*ASF1A/asf1a ASF1B/asf1b*, hereafter *AaBb*), defects were visible in both male and female gametes. Half of the *AaBb* and *aaBb* ovules displayed arrested embryo sacs with functional megaspore identity. Similarly, half of the *AaBb* and *aaBb* pollen grains showed centromere defects, resulting in pollen abortion at the bi-cellular stage of the male gametophyte. However, inheritance of the mutant allele in a given gamete did not solely determine the abortion phenotype. Introducing functional ASF1B failed to rescue the *AaBb*- and *aaBb*-mediated abortion, suggesting that heterozygosity in the *ASF1B* gene causes gametophytic defects, rather than the loss of *ASF1*. The presence of reproductive defects in heterozygous mutants but not in homozygotes, and the characteristic all-or-nothing pollen viability within tetrads, were both indicative of commonly-observed T-DNA-mediated translocation activity for this allele. Our observations reinforce the importance of complementation tests in assigning gene function using reverse genetics.

Keywords: chromosomal rearrangement, gametogenesis, T-DNA insertion

INTRODUCTION

The genome of the dicotyledonous model plant *Arabidopsis thaliana* can be mutagenized using transfer DNA (T-DNA) of the soil bacterium *Agrobacteria tumefaciens*. Plant genome engineering techniques such as these predate CRISPR-Cas9 technology by a quarter of a century (Cong et al., 2013; Feldmann and Marks, 1987; Feldmann et al., 1989; Jinek et al., 2012; Kwon, 2016), and have enabled researchers to link mutant phenotype to genotype, contributing a powerful

Received 25 November, 2019; revised 5 March, 2020; accepted 8 March, 2020; published online 7 April, 2020

eISSN: 0219-1032

and comprehensive catalog of mutations, a tool to plant biologists previously not available in other organisms (O'Malley and Ecker, 2010). Currently more than 700,000 mutant lines with gene affecting insertions have been generated, representing potential disruption mutants for most of the 27,000 *Arabidopsis* genes (Jupe et al., 2019).

The process of T-DNA excision from the tumor inducing (Ti) plasmid and passage through the Agrobacterial membrane is well established; however, the exact mechanism of T-DNA integration into the host genome is not well understood. It is known that multiple T-DNA insertions as direct or inverted repeats occurs frequently during integration, and that this multiple repeat structure often results in intra- and inter-chromosomal rearrangements (Errampalli et al., 1991; Nacry et al., 1998; Thomashow et al., 1980; Ulker et al., 2008; Zambryski et al., 1982; Zhu et al., 2006). In directed T-DNA mutant screens, approximately 17% of the insertion mutants were found to contain chromosomal rearrangements (Castle et al., 1993), although they are often aphenotypic and thus not generally detected. However, there are a number of scenarios whereby T-DNA mediated chromosomal rearrangements can obscure or bias mutant inheritance data, in which case they must be taken into account. For example, intra-chromosomal rearrangements that result in the inversion of chromosomal fragments normally lead to recombination suppression during homologous chromosomal pairing in meiosis. Inter-chromosomal rearrangement results in translocation of the chromosomal fragment and distortion of the linkage group (Curtis et al., 2009). If mutant loci are linked to the rearranged portions of chromosomes, non-Mendelian distribution of segregating populations can be observed during genetic crosses (Clark and Krysan, 2010).

ASF1 is an evolutionarily conserved histone chaperone of the H3/H4 family involved in several fundamental cellular processes, including nucleosome rearrangement and DNA damage repair (English et al., 2005; Le et al., 1997; Mousson et al., 2005; Schulz and Tyler, 2006; Singer et al., 1998). Two Arabidopsis homologues, *ASF1A* and *ASF1B*, are associated with T-DNA mutant lines *asf1a* (CS393977) and *asf1b* (Salk_105822C) that are loss-of function alleles (Zhu et al., 2011). Single homozygous mutants do not have a phenotype, but ASF1 homologues act redundantly, whereby double homozygotes show a drastic inhibition of vegetative and gametophytic growth (Min et al., 2019; Zhu et al., 2011). Here, we describe our observations of mutants that are heterozygous for the *asf1b* T-DNA insertion. We found completely random, non-Mendelian distributions of F2 progeny from selfed F1 double heterozygous plants (*ASF1A/asf1a ASF1B/asf1b* and *asf1a ASF1B/asf1b,* hereafter *AaBb* and *aaBb,* respectively). Our cytological and genetic data showed that inheritance of the mutant allele in the gamete did not determine whether seeds were viable or not. Further, the *AaBb* and *aaBb* abortion phenotypes were not rescued by expression of functional ASF1. Taken together, our results suggest that the gametophytic abortion observed in heterozygotes, but not in homozygotes, is most likely from a T-DNA mediated chromosome rearrangement that includes the *ASF1B* locus.

MATERIALS AND METHODS

Plant material and growth conditions

asf1a and *asf1b* alleles have been described previously (Min et al., 2019). We obtained T-DNA insertion mutants for *ASF1A* and *ASF1B* from the Arabidopsis Biological Resource Center (ABRC): *asf1a-2* (CS393977), *asf1b-1* (Salk_105822C). All *asf1* double mutants (*AaBb, aaBb, Aabb, aabb*) were obtained by crossing the two single mutants and allowing self-pollination. All genotypes were determined by polymerase chain reaction (PCR) analysis and plants were grown in long-day conditions (16-h light/8-h dark) at 22°C with 60% relative humidity.

Seed-set analysis and whole-mount clearing

Seeds, and any undeveloped ovules, were dissected and the number of each counted on a Leica stereoscopic microscope (Leica Microsystems, Germany). For whole mount clearing, pistils of mature FG7 stage and developing siliques were dissected and mounted in a clearing solution containing chloral hydrate in distilled water. Cleared ovules and seeds were observed using an Axio Imager A1 microscope (Carl Zeiss, Germany) under DIC optics and photographed using an AxioCam HRc camera (Carl Zeiss) as previously described (Min et al., 2019).

Analysis of GUS and GFP expression

GUS histochemical analysis was performed as previously described (Yadegari et al., 2000). Female gametophytes from plants expressing GFP fluorescence were analyzed using an LSM700 (Carl Zeiss) confocal laser microscope.

Confocal laser scanning microscopic analysis

For the analysis of embryo sac development in wild type and *asf1* mutants, confocal laser scanning microscopic (CLSM) analysis of ovules was performed as previously described (Min et al., 2019).

Pollen viability analysis using Alexander's staining and DAPI staining

For analysis of pollen viability, pollen grains were mounted with Alexander's staining solution as previously described (Park et al., 2014). To visualize nuclei in pollen grains, DAPI (4′,6-diamidino-2-phenylindole) staining was performed. The Alexander-stained slides and DAPI fluorescence were examined using an Axio Imager A1 microscope under DIC optics and were photographed using an AxioCam HRc camera.

RESULTS

ASF1B/asf1b heterozygosity causes defects during reproduction

The two *Arabidopsis thaliana* ASF1 homologues, *ASF1A* (At1g66740) and *ASF1B* (At5g38110), play redundant roles in replication-dependent chromatin assembly during vegetative and gametophytic growth (Min et al., 2019; Zhu et al., 2011). By crossing the single mutants, *asf1a* and *asf1b* (Supplementary Fig. S1), which do not display developmental defects, *AaBb* double heterozygous plants were generated and

then self-pollinated. The F2 segregating population showed distorted Mendelian segregation (Supplementary Table S1), and the *AaBb* and *aaBb* double mutants displayed distinctly reduced fertility compared to any of the other genotypes (Fig. 1A, Table 1). *aaBb* mutants exhibited 47% seed viability (n = 1,351) (Table 1). Intriguingly, however, self-fertilized *AaBb* double heterozygous plants also showed 52% seed viability (n = 2,009) (Table 1). Approximately half of the ovules from *AaBb* and *aaBb* mutants aborted (47% and 50%, respectively) compared to 8% ovules aborted from *Aabb* plants. This result indicates that, intriguingly, *Bb* heterozygosity is more detrimental to seed viability than the *bb* homozygous state.

Mitotic defects and a failure of proper cell identity during female gametogenesis were observed in *aaBb* and *AaBb* mutants

In *aaBb* and *AaBb* mutants, approximately half of the ovules developed only a short embryo sac and subsequently aborted (Fig. 1B, Table 1). We introduced cell-specific markers (*DD45::GFP* for the egg cell and *DD7::GFP* for the central cell; Steffen et al., 2007) into *aaBb* and *AaBb* mutant plants to ascertain the identity of the cells present within normal and aborting embryo sacs. Normal embryo sacs demonstrated appropriate fluorescence to indicate the correct egg and central cell identities (Figs. 2A-2D); however, arrested ovules did not (Figs. 2E-2H). To determine at which developmental stage the aberrant ovules had aborted, we introduced into *aaBb* and *AaBb* mutants a marker for functional megaspores, the *FM2::GUS* transgene (Olmedo-Monfil et al., 2010). FM2::GUS was not expressed in normal embryo sacs (Figs. 2I and 2J), but was expressed in arrested ovules (Figs. 2K and 2L), indicating that arrested embryo sacs have functional megaspore identity. Hence, meiosis occurred to produce functional haploid megaspores, but the subsequent haploid mitotic divisions, so called megagametogenesis, to produce functional gametes, were not completely processed, thereby a developing embryo sac was impaired in *aaBb* and *AaBb* mutants.

To delineate the cause of ovule arrest in *aaBb* and *AaBb* mutants, we analyzed the development of the female gametophyte using confocal microscopy. Consistent with *FM2:GUS* marker gene expression, no discernible differences during meiotic division were observed within the *aaBb* and *AaBb* mutant ovules. Megagametogenesis of wild-type plants proceeds from FG1 to the FG7 mature female gametophytic stage (Christensen et al., 1997) (Figs. 3A-3C). In contrast, *aaBb* and *AaBb* mutants universally failed to undergo three rounds of haploid mitotic division of the megaspore, resulting in either a single nucleus (no division, Fig. 3E) or two nuclei (one mitotic division; Fig. 3F) inside the short embryo sac. Even though we observed ovules that had reached the FG3

Table 1. Analysis of *ASF1* mutants seed viability

Parental genotypes	Normal seed (%)	Ovule abortion (%)	Seed abortion (%)	Total (n)
AABB	92.5	5.9	1.6	796
aaBB	96.1	3.3	0.7	1,196
AAbb	97	2.3	0.7	881
aaBb	47	49.6	3.4	1,351
Aabb	83.5	7.7	8.8	3,323
AaBb	52.2	47	0.8	2,009

Abortion ratio (%) = (No. of aborted seeds or ovules / No. of total seeds) × 100.

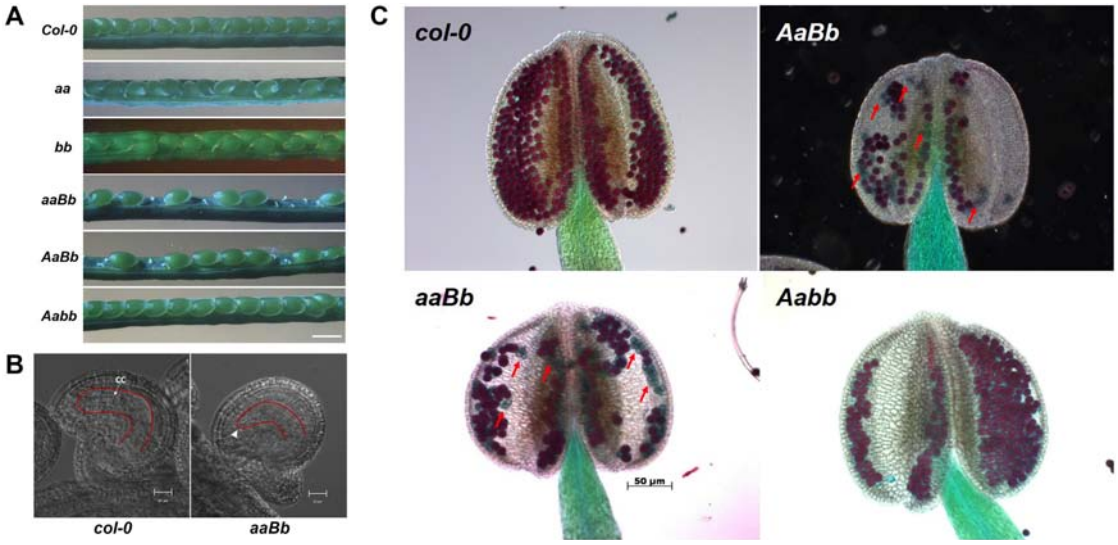

Fig. 1. Comparison of *asf1* mutants during reproduction. (A) Seed formation in wild-type and *asf1* mutant siliques. *aaBb* and *AaBb* siliques showing unfertilised ovules. (B) Wild type (Col-0) ovule and mutant ovule in *aaBb* plants containing an arrested short embryo sac (arrowhead) before fertilization. Red lines indicate embryo sac. CC, central cell. *AaBb* and *aaBb* showed virtually the same phenotype; therefore, we only show *aaBb* here. (C) Alexander staining of a wild-type and *asf1* mutant stamen. Purple stained pollen grains are viable and green shrunken ones are non-viable (arrows). Scale bars = 1 mm (A), 20 μm (B), and 50 μm (C).

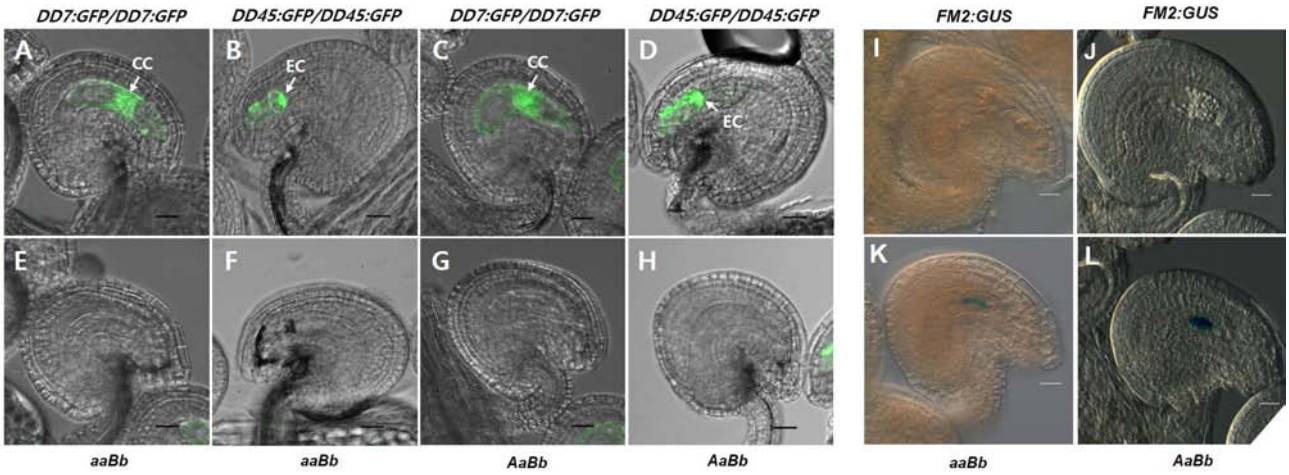

Fig. 2. Arrested *asf1* mutant ovule showed functional megaspore identity. *DD7:GFP* (central cell marker), *DD45:GFP* (egg cell marker), and *FM2:GUS* (functional megaspore marker) transgenes were introduced into *asf1* mutant plants. Images demonstrate the differences between segregating non-arrested (A-D, I and J) and arrested (E-H, K and L) embryo sacs at FG7 stage. (A and E) Ovules from the same pistil of *DD7:GFP/DD7:GFP; aaBb* plants. *DD7:GFP* was not expressed in arrested mutant ovule. (B and F) Ovules from the same pistil of *DD45:GFP/DD45:GFP; aaBb* plants. *DD45:GFP* was not expressed in arrested mutant ovule. (C and G) Ovules from the same pistil of *DD7:GFP/DD7:GFP; AaBb* plants. *DD7:GFP* was not expressed in arrested mutant ovule. (D and H) Ovules from the same pistil of *DD45:GFP/DD45:GFP; AaBb* plants. *DD45:GFP* was not expressed in arrested mutant ovule. (I and K) Ovules from the same pistil of *FM2:GUS/FM2:GUS; aaBb* plants. *FM2:GUS*, absent from segregating mature ovule at FG7 (I), expressed in arrested ovule (K). (J and L) Ovules from the same pistil of *FM2:GUS/FM2:GUS; AaBb* plants. *FM2:GUS*, absent from segregating mature ovule at FG7 (J), expressed in arrested ovule (L). CC, central cell; EC, egg cell. All images are created by merging a DIC image with a GFP image and photographed using confocal microscopy. Scale bars = 20 μm.

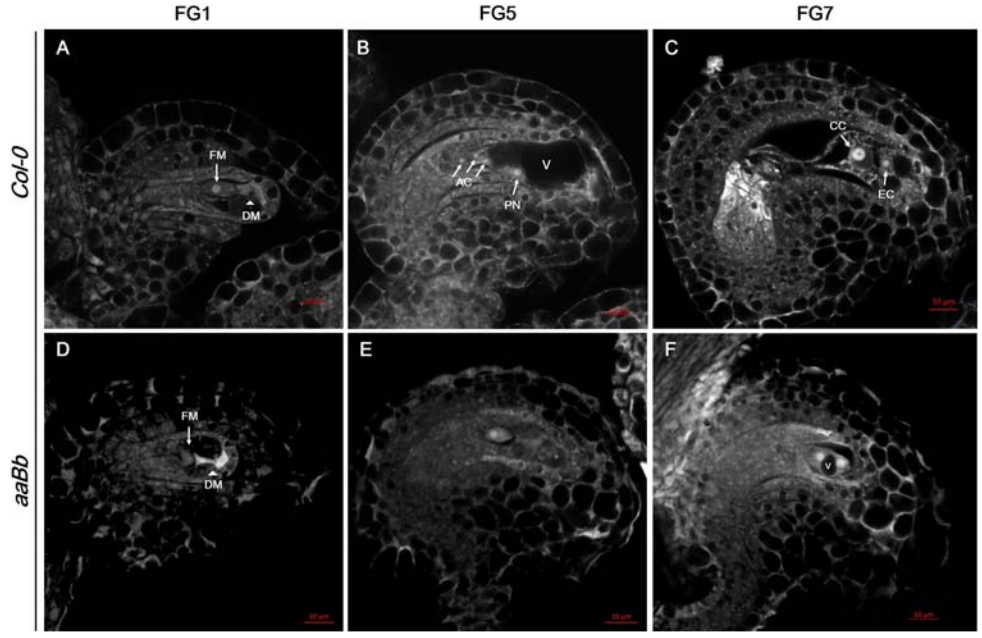

Fig. 3. Defects in female gametogenesis of the *asf1* mutants. (A) Wild-type ovule in the FG1 stage showed meiotic products, functional megaspore (FM, arrow) and degenerated megaspores (DM, arrowhead). (B) Three mitotic divisions from the FM occurred, and an eight-nucleated embryo sac containing a large central vacuole (V) was observed at the FG5 stage. AC, antipodal cell; PN, polar nucleus. (C) Central cell (CC) nucleus by fusion of two polar nuclei was observed. EC, egg cell. (D) *aaBb* mutant ovules displayed abnormal FG1 embryo sacs followed by failure of successive mitotic divisions (E and F). Degenerated nuclei (arrowhead) were identified by their strong autofluorescence. Wild type (top), *aaBb* (bottom) ovules at the same growth period. (A-F) Confocal microscopic images, in which the cytoplasm is displayed as gray, vacuoles as black, and nucleoli as white. Scale bars = 10 μm. *AaBb* and *aaBb* showed virtually the same phenotype in confocal images; therefore, we only show *aaBb* here.

stage (two nuclei and a small vacuole), these did not develop further (Fig. 3F). This phenotype is distinct from that we observed in *aabb* mutants previously, which was shown to be due to the loss of both ASF1A and ASF1B (Min et al., 2019). In these plants, the length of *aabb* embryo sacs were comparable to normal wild-type embryo sacs; therefore, haploid mitotic divisions were occurring, but the subsequent maturation and acquisition of cell identity were defective, resulting in a collapsed embryo sac without visible nuclei in about 30% of the *aabb* ovules (Min et al., 2019). In contrast, ovule arrest in *aaBb* and *AaBb* mutants occurs much earlier than in *aabb* mutants. Taken together, our data indicate that megasporogenesis occurs normally in *aaBb* and *AaBb* mutants, but subsequent mitotic divisions do not proceed beyond the FG3 stage in *aaBb* and *AaBb* mutant ovules.

aaBb and *AaBb* mutants exhibit mitotic defects during male gametogenesis

ASF1 was shown previously to not affect pollen viability, as demonstrated in double *aabb* mutants (Min et al., 2019). Most *aabb* mature pollen grains reached the tri-cellular stage, although subsequent pollen tube elongation was shown to be defective (Min et al., 2019). However, in *aaBb* mutant anthers both viable (purple) and aborted (green) pollen were present when analysed using Alexander's staining (Fig. 1C). In constrast, the viability of *Aabb* pollen was comparable to that of wild-type (Fig. 1C). Similar to our observations in the female gametophyte, the *AaBb* double heterozygote phenotype was identical to *aaBb*, with both viable and aborted pollen present (Fig. 1C), leading us to speculate the mutant *b* allele in the homozygous state, as in *Aabb* mutants, somehow alleviates the phenotype observed in *AaBb* or *aaBb* mutants (Table 1).

To analyze at what stage *aaBb* and *AaBb* pollen arrested, DAPI (4',6-diamidino-2-phenylindole) staining was performed. Virtually all mature wild-type pollen was at the tri-cellular stage with fluorescently stained DNA contained within two sperm nuclei (Fig. 4). However, only half of the pollen from *aaBb* and *AaBb* plants had reached the tri-cellular stage, the rest had shrunk (Fig. 4, asterisks). We determined that although no obvious defects were observed from the diploid pollen mother cell (PMC) to microspore stages prior to pollen mitosis I (PMI), differences between wild type and mutant pollen became apparent during PMI, from the early bi-cellular stage (Fig. 4). *aaBb* and *AaBb* microspores failed to complete PMI (Fig. 4, arrows) exhibiting abnormal pollen morphology with no DAPI staining that quickly became shrunken (Fig. 4, asterisks). This indicated that the *AaBb* and *aaBb* genotypes primarily affect the early stages of male gametophyte development, resulting in a failure of PMI in their half of the pollen.

To visualize mitotic defects in the *AaBb* and *aaBb* pollen, the *ProHTR12:HTR12:GFP* transgene, a centromere marker (Fang and Spector, 2005; Ingouff et al., 2007; Talbert et al., 2002), was introduced into the *AaBb* and *aaBb* mutants by genetic crossing. Then, chromosome segregation during pollen development was observed under the confocal microscope (Fig. 5). In wild-type haploid microspores, HTR12:GFP was detected at all five chromosomal centromeres (Fig. 5A)

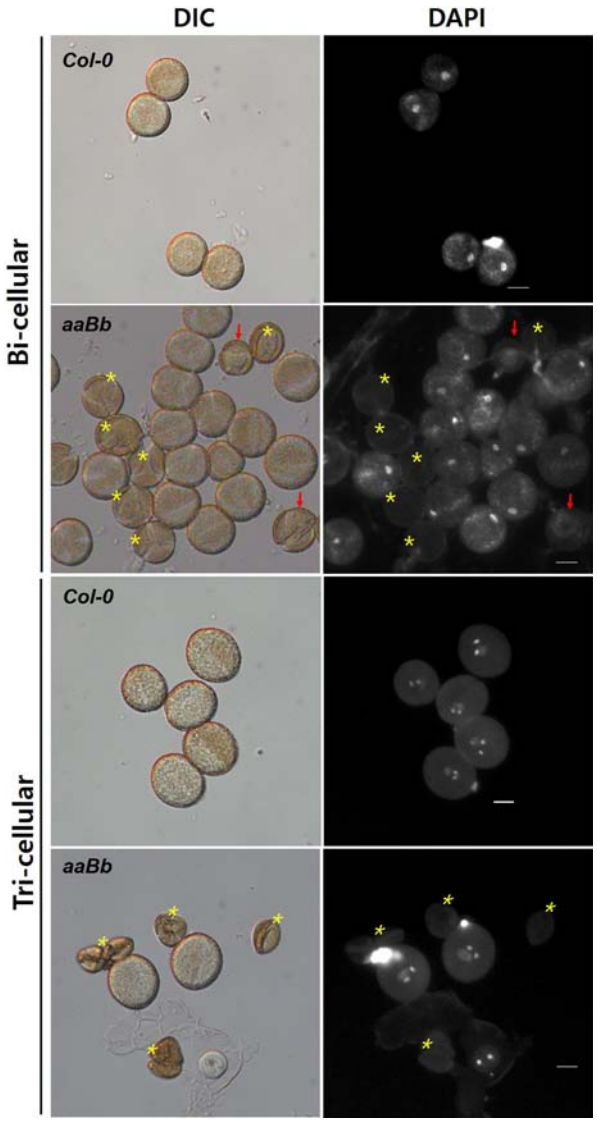

Fig. 4. Pollen development in wild-type plants and *aaBb* mutants. DAPI staining of bi-cellular and tri-cellular stage pollen in wild type and *aaBb* mutants. Note that the bi-cellular stage pollen in *aaBb* mutants is arrested at the microspore stage. The red arrows indicate microspore stage pollen, and the yellow asterisks indicate abnormal pollen with no DAPI staining or shrunken. Scale bars = 10 μm. *AaBb* and *aaBb* showed virtually the same phenotype in confocal images; therefore, we only show *aaBb* here.

and in each dividing cell during PMI (Fig. 5B). Thereafter, GFP was no longer detected in the vegetative cell nucleus (Fig. 5C). Only the generative cell and subsequent sperm cells showed HTR12:GFP expression (Figs. 5C and 5D), as previously reported (Chen et al., 2009) (Fig. 5). *aaBb* and *AaBb* mutant microspores showed an expression pattern similar to that of the wild-type microspores (Figs. 5E and 5I). However, during PMI, HTR12:GFP expression disappeared in half of the pollen grains from the *aaBb* and *AaBb* mutants, and these arrested at the microspore stage without nuclear division (Figs.

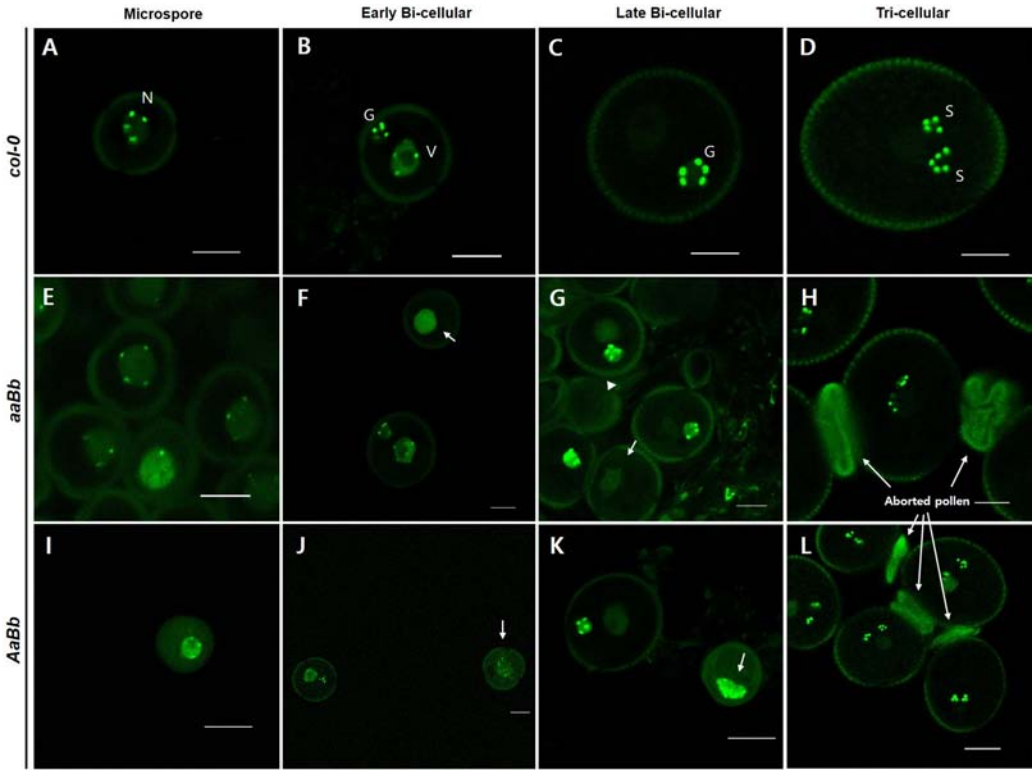

Fig. 5. Defects in male gametogenesis of the *asf1* mutants. HTR12:GFP transgene, a centromere marker observed as a bright dot at the centromere, was introduced into wild type (A-D), *aaBb* (E-H), and *AaBb* (I-L) mutants. Developing pollen grains from wild type (A-D) were photographed using confocal microscopy at the same growth period as *asf1* mutant pollen grains (E-L). (A) Wild-type microspore with bright dots at the centromeres. (B) Early bi-cellular stage after PMI in wild type. (C) Late bi-cellular stage with HTR12:GFP expression only in generative cell in wild type. (D) Tri-cellular stage after PMII with HTR12:GFP expression in two sperms in wild type. (E) Several microspores in *aaBb* mutant. (F) Half of the *aaBb* pollen grains did not show nuclear division with strong fluorescence (arrow). (G) HTR12:GFP expression disappeared from *aaBb* mutant pollen grains (arrowhead) or abnormally detected in the vegetative nucleus, not generative nucleus (arrow). (H) Shrunken pollen grains (arrows) in tri-cellular stage of *aaBb* plants. (I) Microspores in *AaBb* mutants. (J) *AaBb* mutant pollen grains did not show nuclear division (arrow). (K) Arrested *AaBb* mutant pollen grain (arrow). (L) Shrunken pollen grains (arrows) in tri-cellular stage of *AaBb* plants. N, microspore nucleus; G, generative nucleus; V, vegetative nucleus; S, sperm cell nucleus. Scale bars = 10 μm.

5F and 5J, arrows). Occasionally, division did occur in the abnormal pollen grains, with only the vegetative cell nucleus visible (Fig. 5G, arrow), or the pollen appeared empty (Fig. 5G, arrowhead) or had strong staining indicative of being aborted (Fig. 5K, arrow), plus larger more diffuse areas of variegated HTR12 staining (Supplementary Fig. S2). These data demonstrate that progression of the *AaBb* and *aaBb* mutant pollen was prevented through PMI, thus, causing defects in haploid mitosis during pollen development.

Inheritance of the *asf1b* allele does not cosegregate with the defects in female and male gametophytes

In both male and female gametophytes, we observed that *Aabb* mutants exhibited surprisingly higher viability than *AaBb* mutants, which suggested that a possible chromosomal defect had occurred, unlinked to ASF1 gene function. To investigate this, we carried out segregation analysis of the *asf1b* allele. *aaBb* pistils contain approximately 1:1 (50.4% vs 49.6%, n = 1,351) fully matured ovules and small arrested ovules before fertilization (Fig. 1B, Table 1); therefore, we could hypothesize that only either the *aB* or the *ab* female gametophytes generated from *aaBb* pistils would be viable, and could thus undergo fertilization, producing progeny. Thus, either *AaBB* or *AaBb* progeny should survive when *aaBb* pistils were pollinated with wild-type *AABB* pollen. Surprisingly, however, among 152 progeny, we obtained 81 that were *AaBb* and 71 that were *AaBB*, suggesting that female gametophytes inheriting *ab* mutant alleles were fertilized and developed at similar frequencies to *aB* female gametophytes (Table 2). This meant that in *aaBb* pistils, *ab* and *aB* female gametophytes functioned well enough to transmit their alleles. Similarly, both *ab* and *aB* female gametophytes are likely to be present in the aborted ovules. In summary, these data indicate that the *ASF1B* genotype of the female gamete does not determine whether it will be viable or aborted.

During male gametogenesis, we observed many aborted pollen grains in *aaBb* anthers (Figs. 1C and 5H). When we crossed wild-type ovules (*AABB*) with *aaBb* mutant pollen, among 127 F1 progeny, 47 plants were *AaBb* while 80 plants were *AaBB*, meaning that *ab* pollen transmission is reduced

Table 2. Transmission efficiency of the *asf1a* and *asf1b* alleles through reciprocal crosses

Parental genotypes (female × male)	Progeny (n)						
	Aa	AA	Bb	BB	Total (n)	TE_F (%)	TE_M (%)
aaBb × *AABB*	152		81	71	152	114.1	
AABB × *aaBb*	127		47	80	127		58.8

The F1 genotype was determined by PCR. Transmission efficiencies (TE) were calculated as following: TE (%) = No. of progeny with T-DNA insertion / No. of progeny without T-DNA insertion × 100. TE_F, female transmission efficiency; TE_M, male transmission efficiency.

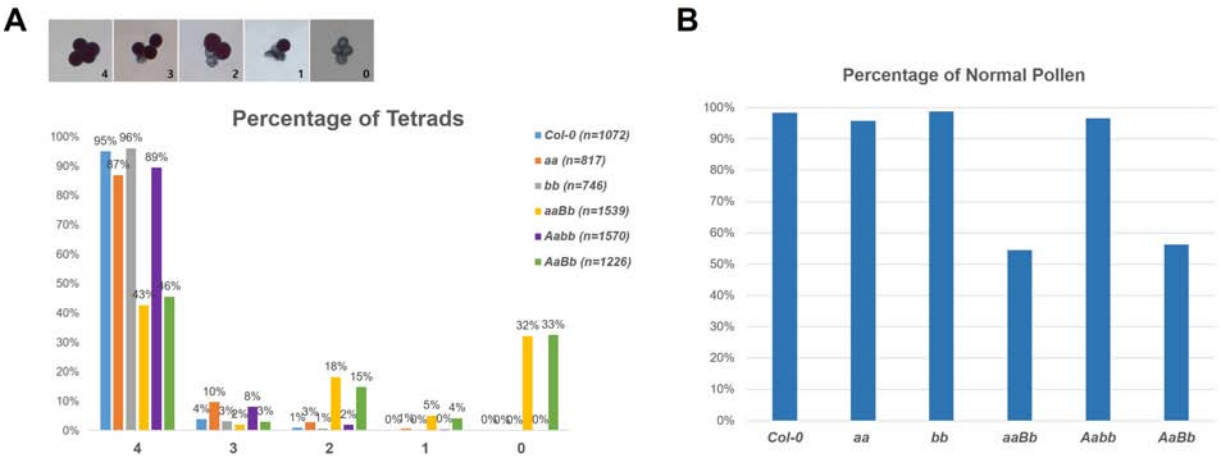

Fig. 6. Pollen viability analysis of *asf1* mutants in a *qrt/qrt* background. (A) Alexander staining and percentage of tetrads containing 4, 3, 2, 1, or 0 normal pollen grains in wild type versus *asf1* mutants. 4, a tetrad of four normal pollen grains; 3, a tetrad of three viable and one aborted pollen grains; 2, a tetrad of two viable and two aborted pollen grains; 1, a tetrad of one viable and three aborted pollen grains; 0, all aborted tetrad. (B) Percentage of total viable pollen in wild-type versus *asf1* mutants.

compared to *aB* pollen (Table 2). Thus, the mutant pollen genotype appears to segregate with mutant phenotype. To further explore the pollen defect and mutant allele segregation, we used *QUARTET* (*qrt*) mutants that fail to undergo microspore separation, releasing viable pollen tetrads (> 95% shown by Alexander Staining; Fig. 6A), allowing us to examine the fate of each of the four progeny from individual PMCs (Preuss et al., 1994). We generated *aaBb*, *Aabb*, and *AaBb* mutant plants in the *qrt1-4* homozygous mutant background by genetic crosses and then analyzed pollen generated from individual PMCs. Compared to wild type, whose pollen grains were virtually all viable, *Aabb* (Fig. 6B, purple bar, n = 1,570) exhibited a slight reduction in viability (89%), reminiscent of the slight reduction in ovule viability in this genotype. Conversely, *aaBb* (Fig. 6B, yellow bar, n = 1,539) and *AaBb* (Fig. 6B, green bar, n = 1,226) mutants showed much lower viability (43% and 46%, respectively) and a distribution of tetrads with all possible viable and nonviable ratios (Fig. 6B). Strikingly, 4:0 viable:nonviable ratios were the most common tetrads in *aaBb* and *AaBb* pollen (43% and 46%, respectively), followed by the tetrads with 0:4 (32% and 33%, respectively). In theory, if *ASF1A* and *ASF1B* are completely redundant, we would expect to get 100% 2:2 viable:nonviable tetrads in *aaBb* and *AaBb* pollen, with their mutations each displaying gametophytic defects during male reproduction. However, we observed only 18% and 15% tetrads with 2:2 ratios in *aaBb* and *AaBb* pollen, respectively. The presence of 4:0 or 0:4 tetrads representing 4 haploid cells that are either all alive, or all dead, in *aaBb* and *AaBb* pollen demonstrate that, in male gametogenesis, neither mutant allele cosegregates with pollen abortion. In addition, the frequent occurrence of 4:0 or 0:4 tetrads is a characteristic feature of two possible results of meiosis-generated reciprocal chromosomal translocations. A cruciform tetravalent can be formed to maximize chromosome paring in a translocation heterozygote. If an alternate disjunction occurs, this can produce euploid gametes, resulting in all 4 viable haploids. If an adjacent disjunction occurs, this produces aneuploid gametes, resulting in all 4 dead pollen grains (Fig. 7). Therefore, our pollen tetrad analysis strongly supports the hypothesis that the observed phenotypes are due to segregation in a translocation heterozygote.

Complementation analysis further suggests that phenotypes observed in the heterozygous *Bb* state are not linked to ASF1 gene function

To examine whether the reproductive phenotypes observed in *AaBb* and *aaBb* were from the T-DNA insertions in *ASF1* genes, we investigated whether the phenotypes were rescued by introducing functional ASF1A or ASF1B. We introgressed *ProASF1A::ASF1A-GFP* and *Pro ASF1B::ASF1B-GFP* transgenic plants (Min et al., 2019) respectively into *AaBb* and *aaBb* mutant backgrounds and analyzed whether the mutant defects were complemented. Surprisingly, neither

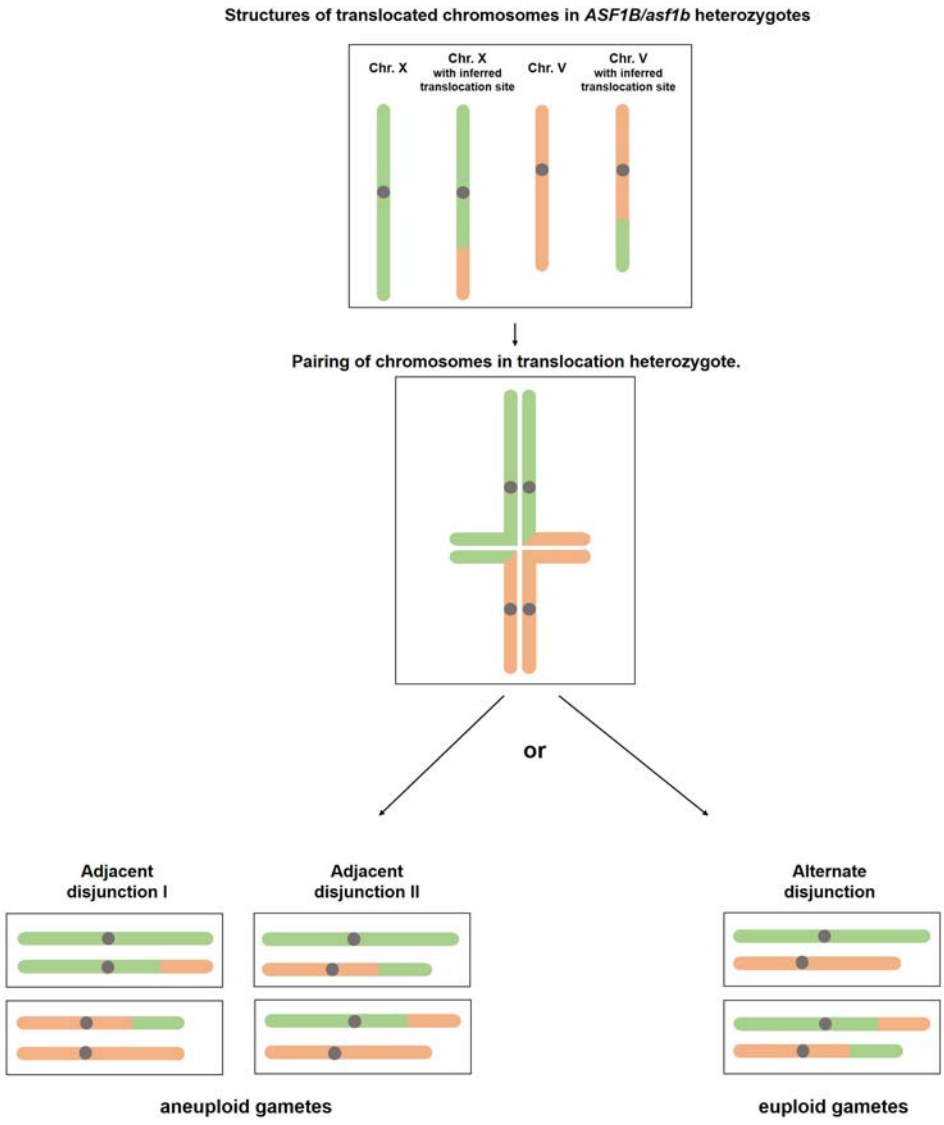

Fig. 7. Plausible structure of translocated chromosomes, meiotic pairing, and subsequent segregation of translocated chromosomes in *ASF1B/asf1b* heterozygotes.

ASF1A-GFP nor ASF1B-GFP, even in the homozygous transgene state, rescued the abortion phenotype (Table 3). This result led us to suspect that lethality might exist in the *Bb* heterozygous state, but not in the *bb* homozygous state, since there was no mutant phenotype observed in *bb* single homozygous plants (Fig. 1A). To confirm this, we crossed *Bb* single heterozygous plants with wild type and their seed set was examined in the progeny. While *BB* wild-type progeny produced virtually all viable seeds, *Bb* single heterozygous plants exhibited 51% (n = 441) ovule abortion (Table 3). Furthermore, the ASF1B-GFP transgene, even in the homozygous state, could not rescue the abortion phenotype of the *Bb* plants (Table 3). These results strongly suggest that the reproductive phenotypes in *AaBb* and *aaBb* plants were not from the T-DNA insertion in the *ASF1B* gene. These data, combined with a lack of Mendelian inheritance of the Bb alleles, and the characteristic meiotic defects that we observe on both the male and female side, suggest that these phenotypes were caused by a T-DNA insertion-mediated

Table 3. *Bb* heterozygous phenotype and complementation analysis

Genotype	Transgene (GFP)	Ovule A %	Seed A %	Total (n)
aaBb	ASF1A/t	46	1	590
	ASF1A/T	43	1	175
AaBb	ASF1A/t	44	0	1,010
	ASF1A/T	47	1	526
aaBb	ASF1B/t	47	6	293
	ASF1B/T	42	4	330
AaBb	ASF1B/t	46	5	1,281
	ASF1B/T	49	5	360
AABb	ASF1B/t	45	11	192
	ASF1B/T	45	13	409
AABb	No transgene	51	0	441
AAbb	No transgene	2.3	0.7	881
AABB	No transgene	3	0	404

chromosome rearrangement. These observations highlight the importance of including complementation analyses when using T-DNA mutants to assign gene function.

DISCUSSION

ASF1 is an evolutionarily conserved histone chaperone required for H3/H4 nucleosome assembly and disassembly and essential cellular processes such as DNA replication, transcription, gene silencing, and DNA damage checkpoint and repair. Previous reports of *ASF1* function in *Arabidopsis* focused on the involvement of ASF1 in vegetative growth and reproductive organ formation, UV-induced DNA damage repair, and heat stress-induced expression of several key heat-shock related genes (Lario et al., 2013; Weng et al., 2014; Zhu et al., 2011). Since the biological function of *ASF1* activity during mega- and microgametogenesis were largely unknown, we aimed to uncover ASF1 function during reproduction using detailed cytological and genetic analyses during sporogenesis, gametogenesis, and seed development.

From single *aa* and *bb* mutants, we generated *AaBb* double heterozygous plants. The *AaBb* plants were then self-fertilized to obtain different combinations of the double mutant genotype. *ASF1A* and *ASF1B* are located on Arabidopsis chromosomes I and V, respectively; therefore, they should show independent assortment in F2 progeny. However, the F2 populations did not show Mendelian segregation (Supplementary Table S1). Moreover, one interesting phenomenon was observed; *aabb* double homozygous plants were underrepresented (dashed-line box in Supplementary Table S2), and *AABB*, *AAbb* and *aaBB* were overrepresented (solid-line box in Supplementary Table S2). The underrepresented *aabb* double homozygous progeny can be explained by an essential but redundant ASF1A and ASF1B function as a histone chaperone during gametogenesis and embryogenesis, so that double homozygous mutant cannot be recovered easily in the F2 progeny (Min et al., 2019).

From *aaBb* plants, *aB* and *ab* alleles were equally transmitted and represented among surviving seeds, even after 50% of the gametes from the female side were dead. We also observed Mendelian segregation among the reduced number of progeny in the selfed *Bb* heterozygotes or *Bb* heterozygous plants crossed reciprocally with wild type. *Bb* heterozygous plants show 50% seed abortion but homozygous *bb* plants produce all viable seeds. This is in contrast to the typical gametophytic or embryonic lethal genes which show reduced transmission and thus underrepresentation of those alleles among the surviving seeds.

The phenotype we observe in *AaBb* and *aaBb* mutants is dominated by a failure of post-meiotic cell divisions during both male and female gametogenesis. On the female side, ovules were aborted with short embryo sacs and functional megaspore identity. During male gametophyte development, pollen grains were arrested and shrunken, having failed to undergo nuclear division. A similar 50% post-meiotic arrest and gamete abortion was previously reported in *Atrev3-2* heterozygous plants (Curtis et al., 2009). AtREV3 (*Arabidopsis thaliana* Recovery protein3) encodes a catalytic subunit of DNA polymerase zeta involved in UVB-induced DNA damage repair by translesion synthesis. Heterozygous *Atrev3-2* plants exhibited 50% ovule and pollen grain abortion, resulting in a 50% reduction of the seed set. The surviving 50% plants displayed a Mendelian distribution of mutant alleles, with a 1:2:1 ratio of wild type:heterozygous *Atrev3-2*:homozygous *Atrev3-2*. Since the reduced seed set (but Mendelian distribution of the progeny) in selfed *Atrev3-2* heterozygotes, but not in homozygotes, was observed, the authors hypothesized that a T-DNA-mediated translocation might have occurred that is associated with the *Atrev3-2* allele, located in chromosome V. They examined chromosome spreads using fluorescence in situ hybridization (FISH) in meiocytes and showed that a tetravalent was formed between chromosome I and V. This indicates that a reciprocal translocation of chromosomal fragments had occurred between chromosomes I and V, leading to the pairing of four chromosomes to form a cruciform structure during meiosis. Two modes of segregation are then possible, with the gametes resulting from adjacent segregation being all sub-haploid, and thus inviable; and those resulting from alternate segregation all being viable (Fig. 7). In the current study, the overrepresented genotypes from our mutant allele segregation analyses; *AABB*, *AAbb*, and *aaBB*, were homozygous for each allele of *ASF1A* and *ASF1B* gene, with either both alleles occurring in the wild type (*AA*, *BB*) or mutant (*aa*, *bb*) state. This means that when undergoing meiosis, homologous chromosomes can pair successfully, even if they contain rearranged chromosomal fragments. The reduced viability and seed set in *Bb* heterozyotes but not in *bb* homozygotes (but with Mendelian segregation) suggests a strong possibility of a translocation of the chromosomal fragment associated with the *asf1b* allele. In our quartet analysis, the two most common phenotype distributions were all 4 viable pollen grains (43% in *aaBb* and 46% in *AaBb*) but also all 4 dead pollen grains (32% in *aaBb* and 33% in *AaBb*). This strongly supports the possibility that a T-DNA associated reciprocal translocation occurred associated with the *asf1b* allele in chromosome V, thereby forming a tetravalent cruciform structure in *asf1b* meiocytes. When alternate segregation occurs, then we see all 4 meiotic products viable (4 purple pollen grains in Fig. 6A), and if adjacent segregation occurs, then we see all 4 pollen grains dead (4 green pollen grains in Fig. 6A). To directly uncover the precise structural abnormalities in *Bb* meiocytes, further experimentation including microscopic observations by FISH and immunolocalization experiments, or genome-wide genetic mapping, could be carried out.

ASF1A and ASF1B proteins are both expressed from the beginning of male and female gamete formation, whereby they are present in the PMC and megaspore mother cell (MMC), and then expressed throughout gametogenesis (Min et al., 2019). Since their expression patterns and the defects of both genuine ASF1 mutant plants (*aabb* mutants), and plants we suspect to have a translocation (*AaBb* and *aaBb* mutants), are overlapping, without performing complementation tests, we could have mis-assigned the role of ASF1 during reproduction. T-DNA-associated chromosomal rearrangement is not uncommon; therefore, our observations further highlight the importance of complementation tests and the use of multiple mutant alleles where possible.

Note: Supplementary information is available on the Molecules and Cells website (www.molcells.org).

ACKNOWLEDGMENTS

The work was supported by NRF of Korea (2017R1A2B2007067) and the Next-Generation BioGreen 21 Program Grant (PJ013127). Y.M. was supported by the Stadelmann-Lee Scholarship Fund, Seoul National University.

AUTHOR CONTRIBUTIONS

Y.M. and Y.C. conceived and designed the experiments. Y.M. performed the experiments. Y.M., J.M.F., and Y.C. analyzed the data and wrote the paper.

CONFLICT OF INTEREST

The authors have no potential conflicts of interest to disclose.

ORCID

Yunsook Min https://orcid.org/0000-0002-7531-7809
Jennifer M. Frost https://orcid.org/0000-0002-3057-6313
Yeonhee Choi https://orcid.org/0000-0002-2796-5262

REFERENCES

Castle, L.A., Errampalli, D., Atherton, T.L., Franzmann, L.H., Yoon, E.S., and Meinke, D.W. (1993). Genetic and molecular characterization of embryonic mutants identified following seed transformation in Arabidopsis. Mol. Gen. Genet. *241*, 504-514.

Chen, Z., Hafidh, S., Poh, S.H., Twell, D., and Berger, F. (2009). Proliferation and cell fate establishment during Arabidopsis male gametogenesis depends on the Retinoblastoma protein. Proc. Natl. Acad. Sci. U. S. A. *106*, 7257-7262.

Christensen, C.A., King, E.J., Jordan, J.R., and Drews, G.N. (1997). Megagametogenesis in Arabidopsis wild type and the Gf mutant. Sex. Plant Reprod. *10*, 49-64.

Clark, K.A. and Krysan, P.J. (2010). Chromosomal translocations are a common phenomenon in Arabidopsis thaliana T-DNA insertion lines. Plant J. *64*, 990-1001.

Cong, L., Ran, F.A., Cox, D., Lin, S., Barretto, R., Habib, N., Hsu, P.D., Wu, X., Jiang, W., Marraffini, L.A., et al. (2013). Multiplex genome engineering using CRISPR/Cas systems. Science *339*, 819-823.

Curtis, M.J., Belcram, K., Bollmann, S.R., Tominey, C.M., Hoffman, P.D., Mercier, R., and Hays, J.B. (2009). Reciprocal chromosome translocation associated with TDNA-insertion mutation in Arabidopsis: genetic and cytological analyses of consequences for gametophyte development and for construction of doubly mutant lines. Planta *229*, 731-745.

English, C.M., Maluf, N.K., Tripet, B., Churchill, M.E.A., and Tyler, J.K. (2005). ASF1 binds to a heterodimer of histories H3 and H4: a two-step mechanism for the assembly of the H3-H4 heterotetramer on DNA. Biochemistry *44*, 13673-13682.

Errampalli, D., Patton, D., Castle, L., Mickelson, L., Hansen, K., Schnall, J., Feldmann, K., and Meinke, D. (1991). Embryonic lethals and T-DNA insertional mutagenesis in Arabidopsis. Plant Cell *3*, 149-157.

Fang, Y. and Spector, D.L. (2005). Centromere positioning and dynamics in living Arabidopsis plants. Mol. Biol. Cell *16*, 5710-5718.

Feldmann, K.A. and Marks, M.D. (1987). Agrobacterium-mediated transformation of germinating seeds of Arabidopsis thaliana: a non-tissue culture approach. Mol. Gen. Genet. *208*, 1-9.

Feldmann, K.A., Marks, M.D., Christianson, M.L., and Quatrano, R.S. (1989). A dwarf mutant of Arabidopsis generated by T-DNA insertion mutagenesis. Science *243*, 1351-1354.

Ingouff, M., Hamamura, Y., Gourgues, M., Higashiyama, T., and Berger, F. (2007). Distinct dynamics of HISTONE3 variants between the two fertilization products in plants. Curr. Biol. *17*, 1032-1037.

Jinek, M., Chylinski, K., Fonfara, I., Hauer, M., Doudna, J.A., and Charpentier, E. (2012). A programmable dual-RNA-guided DNA endonuclease in adaptive bacterial immunity. Science *337*, 816-821.

Jupe, F., Rivkin, A.C., Michael, T.P., Zander, M., Motley, S.T., Sandoval, J.P., Slotkin, R.K., Chen, H., Castanon, R., Nery, J.R., et al. (2019). The complex architecture and epigenomic impact of plant T-DNA insertions. PLoS Genet. *15*, e1007819.

Kwon, T. (2016). Mitochondrial porin isoform AtVDAC1 regulates the competence of Arabidopsis thaliana to Agrobacterium-mediated genetic transformation. Mol. Cells *39*, 705-713.

Lario, L.D., Ramirez-Parra, E., Gutierrez, C., Spampinato, C.P., and Casati, P. (2013). ANTI-SILENCING FUNCTION1 proteins are involved in ultraviolet-induced DNA damage repair and are cell cycle regulated by E2F transcription factors in Arabidopsis. Plant Physiol. *162*, 1164-1177.

Le, S.Y., Davis, C., Konopka, J.B., and Sternglanz, R. (1997). Two new S-phase-specific genes from Saccharomyces cerevisiae. Yeast *13*, 1029-1042.

Min, Y., Frost, J.M., and Choi, Y. (2019). Nuclear chaperone ASF1 is required for gametogenesis in Arabidopsis thaliana. Sci. Rep. *9*, 13959.

Mousson, F., Lautrette, A., Thuret, J.Y., Agez, M., Courbeyrette, G., Amigues, B., Becker, E., Neumann, J.M., Guerois, R., Mann, C., et al. (2005). Structural basis for the interaction of Asf1 with histone H3 and its functional implications. Proc. Natl. Acad. Sci. U. S. A. *102*, 5975-5980.

Nacry, P., Camilleri, C., Courtial, B., Caboche, M., and Bouchez, D. (1998). Major chromosomal rearrangements induced by T-DNA transformation in Arabidopsis. Genetics *149*, 641-650.

Olmedo-Monfil, V., Duran-Figueroa, N., Arteaga-Vazquez, M., Demesa-Arevalo, E., Autran, D., Grimanelli, D., Slotkin, R.K., Martienssen, R.A., and Vielle-Calzada, J.P. (2010). Control of female gamete formation by a small RNA pathway in Arabidopsis. Nature *464*, 628-632.

O'Malley, R.C. and Ecker, J.R. (2010). Linking genotype to phenotype using the Arabidopsis unimutant collection. Plant J. *61*, 928-940.

Park, G.T., Frost, J.M., Park, J.S., Kim, T.H., Lee, J.S., Oh, S.A., Twell, D., Brooks, J.S., Fischer, R.L., and Choi, Y. (2014). Nucleoporin MOS7/Nup88 is required for mitosis in gametogenesis and seed development in Arabidopsis. Proc. Natl. Acad. Sci. U. S. A. *111*, 18393-18398.

Preuss, D., Rhee, S.Y., and Davis, R.W. (1994). Tetrad analysis possible in Arabidopsis with mutation of the QUARTET (QRT) genes. Science *264*, 1458-1460.

Schulz, L.L. and Tyler, J.K. (2006). The histone chaperone ASF1 localizes to active DNA replication forks to mediate efficient DNA replication. FASEB J. *20*, 488-490.

Singer, M.S., Kahana, A., Wolf, A.J., Meisinger, L.L., Peterson, S.E., Goggin, C., Mahowald, M., and Gottschling, D.E. (1998). Identification of high-copy disrupters of telomeric silencing in Saccharomyces cerevisiae. Genetics *150*, 613-632.

Snustad, D.P. and Simmons, M.J. (2016). Principles of Genetics (Hoboken, NJ: John Wiley & Sons).

Steffen, J.G., Kang, I.H., Macfarlane, J., and Drews, G.N. (2007). Identification of genes expressed in the Arabidopsis female gametophyte. Plant J. *51*, 281-292.

Talbert, P.B., Masuelli, R., Tyagi, A.P., Comai, L., and Henikoff, S. (2002). Centromeric localization and adaptive evolution of an Arabidopsis histone H3 variant. Plant Cell *14*, 1053-1066.

Thomashow, M.F., Nutter, R., Montoya, A.L., Gordon, M.P., and Nester, E.W. (1980). Integration and organization of Ti plasmid sequences in crown gall tumors. Cell *19*, 729-739.

Ulker, B., Peiter, E., Dixon, D.P., Moffat, C., Capper, R., Bouche, N., Edwards,

R., Sanders, D., Knight, H., and Knight, M.R. (2008). Getting the most out of publicly available T-DNA insertion lines. Plant J. *56*, 665-677.

Weng, M., Yang, Y., Feng, H., Pan, Z., Shen, W.H., Zhu, Y., and Dong, A. (2014). Histone chaperone ASF1 is involved in gene transcription activation in response to heat stress in Arabidopsis thaliana. Plant Cell Environ. *37*, 2128-2138.

Yadegari, R., Kinoshita, T., Lotan, O., Cohen, G., Katz, A., Choi, Y., Nakashima, K., Harada, J.J., Goldberg, R.B., Fischer, R.L., et al. (2000). Mutations in the FIE and MEA genes that encode interacting polycomb proteins cause parent-of-origin effects on seed development by distinct mechanisms. Plant Cell *12*, 2367-2381.

Zambryski, P., Depicker, A., Kruger, K., and Goodman, H.M. (1982). Tumor induction by Agrobacterium tumefaciens: analysis of the boundaries of T-DNA. J. Mol. Appl. Genet. *1*, 361-370.

Zhu, Q.H., Ramm, K., Eamens, A.L., Dennis, E.S., and Upadhyaya, N.M. (2006). Transgene structures suggest that multiple mechanisms are involved in T-DNA integration in plants. Plant Sci. *171*, 308-322.

Zhu, Y., Weng, M., Yang, Y., Zhang, C., Li, Z., Shen, W.H., and Dong, A. (2011). Arabidopsis homologues of the histone chaperone ASF1 are crucial for chromatin replication and cell proliferation in plant development. Plant J. *66*, 443-455.